

THEORETICAL STUDIES OF
DIELECTRIC SUSCEPTIBILITY IN
FERROELECTRIC THIN FILM

by

SIA CHEN HOW

Thesis submitted in fulfillment of
the requirements for the degree of
Master of Science

UNIVERSITI SAINS MALAYSIA

DECEMBER 2007

ACKNOWLEDGEMENTS

My sincere appreciation to my supervisors, Prof. Dr. Junaidah Osman and Dr. Ong Lye Hock, for their guidance and suggestions throughout the whole process of my study. I also would like to express heartiest gratitude to Prof. Yoshihiro Ishibashi for his invaluable advice and suggestions.

I am grateful to my family, parents, brothers, sister, friends and my colleagues for their constant encouragement and support.

TABLE OF CONTENTS

	Page
ACKNOWLEDGEMENTS	ii
TABLE OF CONTENTS	iii
LIST OF TABLES	v
LIST OF FIGURES	vi
ABSTRAK	x
ABSTRACT	xii
CHAPTER 1 GENERAL INTRODUCTION	
1.1 Introduction	1
1.2 Motivation of Study	1
1.3 Organization of Contents	2
1.4 Past and Present of Ferroelectricity	3
1.5 Definition of Ferroelectricity	6
1.6 Classification of Ferroelectric Materials	7
1.6.1 Displacive Ferroelectrics	9
1.6.2 Order-Disorder Ferroelectrics	12
1.7 Properties of Ferroelectric materials	14
1.7.1 Hysteresis Loop and Polarization Switching	14
1.7.2 Dielectric and Susceptibility	17
1.7.3 Domains	20
1.7.4 The Phase Transition	23
1.8 Crystal Structure	25
1.9 Applications of Ferroelectric Materials	27
1.9.1 Dielectric Applications	27
1.9.2 Pyroelectric Applications	29
1.9.3 Piezoelectric Applications	30
1.9.4 Electro-optic Applications	31
1.9.5 Polarization Applications	32
CHAPTER 2 THEORIES AND REVIEWS OF FERROELECTRICS	
2.1 Introduction	34
2.2 Microscopic Theory: Soft Mode	34
2.3 Macroscopic Theory: The Landau Theory	36
2.3.1 Second Order Ferroelectric Phase Transitions	38
2.3.1.1 Free Energy Function	38

2.3.1.2	The Dielectric Susceptibility for Second-Order Ferroelectrics	41
2.3.2	First-Order Ferroelectric Phase Transitions	42
2.3.2.1	Free Energy Function	42
2.3.2.2	The Dielectric Susceptibility for First-order Ferroelectrics	48
2.4	The Finite-Size Effects in Ferroelectric Thin Films	49
2.4.1	Experimental Review	50
2.4.2	Theoretical Review	52
2.5	Formulation of The Free Energy Function in Ferroelectric Films	55
CHAPTER 3 CALCULATION OF DIELECTRIC SUSCEPTIBILITY IN		
FERROELECTRIC THIN FILMS		
3.1	Introduction	58
3.2	Zero Surface Polarization, $p_{\pm} = 0$	59
3.2.1	Calculation For Zero Surface Polarization Case	59
3.2.2	Results and Discussions	62
3.3	Non-zero Surface Polarization, $p_{\pm} \neq 0$	68
3.3.1	Calculation For Non-zero Surface Polarization Case	68
3.3.2	Results and Discussions	72
CHAPTER 4 DISCRETE MODEL OF DIELECTRIC SUSCEPTIBILITY IN		
FERROELECTRIC THIN FILMS		
4.1	Introduction	80
4.2	Second Order Thin Films with Zero Surface Polarization $p_{\pm} = 0$	80
4.2.1	Theory and Modelling For Zero Surface Polarization Case	80
4.2.2	Numerical Results	83
4.3	Second Order Thin Films with Non-Zero Surface Polarization $p_{\pm} \neq 0$	89
4.3.1	Theory and Modelling For Non-zero Surface Polarization Case	89
4.3.2	Numerical Results	92
CHAPTER 5 CONCLUSION AND DISCUSSION		101
REFERENCES		103
LIST OF PUBLICATION		111
APPENDICES		

LIST OF TABLES

	Page
1.1 Important events in ferroelectricity (Cross and Newnham, 2003)	5
1.2 Displacive and order-disorder ferroelectric materials (Kittel, 1986)	7
1.3 Some common ferroelectric materials (Auciello, 1998).	8

LIST OF FIGURES

	Page
1.1 Rochelle salt hysteresis loop obtained by J. Valasek. (Valasek 1920)	4
1.2 A ferroelectric is a polar material whose spontaneous polarization can be reversed or re-oriented by applying electric field. A simple illustration of a ferroelectric material (figure courtesy of Symetrix Corporation).	6
1.3 Common elements, marked in shaded area, in displacive type of ferroelectric crystal (Richerson, 1992).	9
1.4 Lattice with perovskite structure having formula ABO_3 . "A" atom, "B" atom, and oxygen occupy the corner site, body-centered site, and face-centered site, respectively (A.F Wells, 1995).	10
1.5 Different symmetry axes directions (A.F. Wells, 1995).	11
1.6 The perovskite structure ABO_3 of $PbTiO_3$ in a) paraelectric and b) ferroelectric phase (Damjanovic, 1998).	12
1.7 Schematic representation of the system of hydrogen bonds in KH_2PO_4 (KDP) crystals. The PO_4 groups with hydrogen bonds link to the nearest PO_4 groups (Zhong, 1998).	13
1.8 a) the simplest electric circuit for observation of the dependence of electric polarization on electric (Sawyer-Tower circuit) and b) the shape of voltage applied to crystal (Sawyer and Tower, 1969).	15
1.9 Schematic illustration of the $P-E$ hysteresis loop. Ellipses with arrows show the polarization of the crystal (Sawyer and Tower, 1969).	16
1.10 Schematic illustration of the nucleation and growth process during polarization switching (Chew, 2001).	17
1.11 Temperature dependence of $\varepsilon(T)$ a) first order transition and b) second order transition.	18
1.12 The dielectric constant $\varepsilon(T)$ of $BaTiO_3$ crystal. ε_c is the dielectric constant along the polar axis and ε_a perpendicular to the axis (Uchino, 2000)	19
1.13 Effect of poling on dipole orientation (Damjanovic, 1998).	20
1.14 Formation of and domain wall in a tetragonal perovskite ferroelectric phase (Damjanovic, 1998).	21
1.15 A simple sketch of domain walls: (a) 180° (b) 90° (Zhong, 1998).	22

1.16	Ferroelectric phase transitions in the vicinity of the Curie temperature T_C . The temperature dependence of P_s : (a) first-order transition and (b) second-order transition (Blinc and Zeks, 1974).	24
1.17	Schematic illustration of the temperature dependence of the spontaneous polarization for BaTiO_3 (Uchino, 2000).	25
1.18	Relationship between piezoelectricity, pyroelectricity and ferroelectricity. a) Relationship between crystal classes and piezoelectric, pyroelectric and ferroelectric properties. b) Specific crystal classes for piezoelectric and pyroelectric materials together with their general optical response. Note: 432 is not piezoelectric (Richerson, 1992).	26
1.19	The relationship between (a) P vs. E , (b) C vs. V and (c) I vs. V for a ferroelectric capacitor. (McMillan, 2005)	28
1.20	Changing dimension of crystal structure in applied external electric field (http://www.physikinstrumente.com/tutorial/ , 2008).	30
2.1	The free energy g versus polarization p for second-order bulk ferroelectric system without external field where the temperatures are: $t = 0.0$, $t = 0.5$, $t = 1.0$, $t = 1.5$.	39
2.2	Spontaneous polarization of second-order ferroelectric. Curves a and b correspond to field strength of $e = 0.0$ and $e = 0.03$ respectively.	40
2.3	Static dielectric constant versus temperature for second-order ferroelectric. The ratio of the slope magnitudes above and below $t = 1.0$ equals to 2.	41
2.4	Temperature dependence of the free energy g versus polarization p for first-order bulk ferroelectric system in the absence of external electric field where each curve corresponds to different reduced temperature: $t = -0.5, 0.0, 0.375, 0.75, 0.875, 1.0, 1.4, 1.8$ and 2.0 .	44
2.5	Spontaneous polarization of first order ferroelectric versus temperature. Curve a and b correspond to field strength with $e = 0.0$ and $e = 0.20$ respectively. Solid lines represent both local and global stable states while dashed lines represent unstable states.	47
2.6	Static dielectric constant versus temperature for first order ferroelectric. The discontinuity at t_c signifies the first order nature of the transition.	48
2.7	Variation of the local polarization $P(z)$ in the vicinity of a plane surface situated at $z = 0$ (Zhong, 1998).	56
3.1	Polarization profile in FE film with thickness, l	60
3.2	Polarization profile $p(\zeta)$ versus distance ζ in FE film with thickness $l=5$.	62

3.3	Polarization profile $p(\zeta)$ versus distance ζ in FE film at temperature $t=0.4$.	63
3.4	Polarization profile $p(\zeta)$ versus distance ζ for FE film in different applied electric field.	63
3.5	(a) Dielectric susceptibility χ'_T versus temperature t and (b) Reciprocal dielectric susceptibility $1/\chi'_T$ versus temperature t in FE film for different thickness l .	66
3.6	(a) Dielectric susceptibility χ'_T versus inverse thickness $1/l^2$ and (b) Reciprocal dielectric susceptibility $1/\chi'_T$ versus inverse thickness $1/l^2$ in FE film for different temperature t .	67
3.7	Polarization profile in FE film with thickness l and extrapolation length η .	69
3.8	Polarization profile in FE film with thickness $l=5$ and extrapolation length $\eta=2$.	72
3.9	Polarization profile in FE film with extrapolation length $\eta=2$ at temperature $t=0.5$.	73
3.10	Polarization profile in FE film with thickness $l=2$ at temperature $t=0.5$.	73
3.11	(a) Dielectric susceptibility χ'_T versus temperature t and (b) Reciprocal dielectric susceptibility $1/\chi'_T$ versus temperature t in FE film with extrapolation length $\eta=2$ for different thickness l	76
3.12	(a) Dielectric susceptibility χ'_T versus temperature t and (b) Reciprocal dielectric susceptibility $1/\chi'_T$ versus temperature t in FE film in thickness $l=2$ for different extrapolation length η .	77
3.13	(a) Dielectric susceptibility χ'_T versus inverse thickness $1/l$ and (b) Reciprocal dielectric susceptibility $1/\chi'_T$ versus inverse thickness $1/l$ in FE film with thickness $\eta=2$ for different temperature t .	78
3.14	(a) Dielectric susceptibility χ'_T versus inverse thickness $1/l$ and (b) Reciprocal dielectric susceptibility $1/\chi'_T$ versus inverse thickness $1/l$ in FE film at temperature $t=0.5$ for different extrapolation length η .	79
4.1	Three sector values on initial polarization profile is computed to yield the new polarization value of the next step.	82

4.2	Polarization profile $p(\zeta)$ versus distance ζ in FE film with thickness $l=5$.	84
4.3	Polarization profile $p(\zeta)$ versus distance ζ in FE film at temperature $t=0.4$.	84
4.4	(a) Dielectric susceptibility χ'_T versus temperature t and (b) Reciprocal dielectric susceptibility $1/\chi'_T$ versus temperature t in FE film for different thickness l .	87
4.5	(a) Dielectric susceptibility χ'_T versus inverse thickness $1/l^2$ and (b) Reciprocal dielectric susceptibility $1/\chi'_T$ versus inverse thickness $1/l^2$ in FE film for different temperature t .	88
4.6	The polarization value p_i and the spatial differential of polarization s_i is evaluated to obtain the new polarization value of the next sector p_{i+1} .	91
4.7	Polarization profile in FE film with extrapolation length $\eta=1$ and thickness $l=2$.	92
4.8	Polarization profile in FE film with extrapolation length $\eta=1$ at temperature $t=0.5$.	93
4.9	Polarization profile in FE film with thickness $l=2$ at temperature $t=0.5$.	94
4.10	(a) Dielectric susceptibility χ'_T versus temperature t and (b) Reciprocal dielectric susceptibility $1/\chi'_T$ versus temperature t in FE film with extrapolation length $\eta=1$ for different thickness l .	97
4.11	(a) Dielectric susceptibility χ'_T versus temperature t and (b) Reciprocal dielectric susceptibility $1/\chi'_T$ versus temperature t in FE film with thickness $l=3$ for different extrapolation length η .	98
4.12	(a) Dielectric susceptibility χ'_T versus inverse thickness $1/l$ and (b) Reciprocal dielectric susceptibility $1/\chi'_T$ versus inverse thickness $1/l$ in FE film with extrapolation length $\eta=1$ for different temperature t .	99
4.13	(a) Dielectric susceptibility χ'_T versus inverse thickness $1/l$ and (b) Reciprocal dielectric susceptibility $1/\chi'_T$ versus inverse thickness $1/l$ in FE film at temperature $t=0.6$ for different extrapolation length η .	100

KAJIAN TEORI BAGI KERENTANAN DIELEKTRIK DALAM FILEM NIPIS FERROELEKTRIK

ABSTRAK

Kerentanan dielektrik bagi filem nipis ferroelektrik (FE) bawah peralihan fasa tertib kedua dikajikan dengan rangkakerja tenaga bebas Landau-Devonshire. Huraian yang teliti ditunjukkan untuk mendapatkan kerentanan dielektrik bagi filem ferroelektrik dalam fasa paraelektrik $T > T_C$ dan fasa ferroelektrik $T < T_C$ (T_C ialah suhu kritikal). Filem nipis ferroelektrik dianggap simetri dengan ketebalan L , dari $-L/2$ ke $L/2$ di paksi z . Fungsi cubaan trigonometri digunakan untuk mewakili profil pengutuban dalam filem nipis. Ciri-ciri bagi ferroelektrik filem nipis di dalam fasa peralihan dikaji dengan menggunakan tenaga bebas bagi model Tilley-Zeks dan tenaga bebas Landau-Devonshire. Densiti tenaga bebas dinilai dan dikirakan mendapat huraian kerentanan dielektrik. Selepas meminimumkan tenaga bebas terhadap pengutuban dan menggunakan $\chi_T^{-1} = \partial E / \partial P$, kerentanan dielektrik diperolehi. Kelakuan bagi kerentanan dielektrik dalam filem nipis ferroelektrik dikajikan di bawah pelbagai kesan ketebalan, suhu dan keadaan sempadan. Untuk kajian kes, dua fungsi cubaan digunakan bagi pengutuban permukaan sifar $P_{\pm} = 0$ and bagi pengutuban permukaan bukan sifar $P_{\pm} \neq 0$.

Langkah numerikal juga ditunjukkan untuk memberikan sokongan lanjut bagi keputusan pengkiraan. Model diskret juga berdasarkan rangkakerja tenaga bebas Landau-Devonshire dalam sebutan pengutuban. Profil pengutuban bagi filem nipis ditentukan dan pengutuban purata dinilai untuk mengkira kerentanan dielektrik. Keputusan dari dua keadaan sempadan yang berbeza, pengutuban permukaan sifar dan pengutuban bukan sifar, dibandingkan dengan keputusan pengkiraan.

Didapati bahawa keputusan pengkiraan dan keputusan numerikal adalah tepat untuk menghuraikan ciri-ciri persandaran suhu dan ketebalan dielektrik bagi filem nipis

FE tertib kedua. Keputusan juga menunjukkan kerentanan dielektrik bergantung kepada panjang ekstrapolasi and keadaan sempadan.

THEORETICAL STUDIES OF DIELECTRIC SUSCEPTIBILITY IN FERROELECTRIC THIN FILM

ABSTRACT

The dielectric susceptibility of ferroelectric (FE) thin film in the second-order phase transition is under study within the framework of the Landau-Devonshire free energy expansion. A detailed derivation is presented to find the dielectric susceptibility of a ferroelectric film in the paraelectric phase $T > T_C$ and ferroelectric phase $T < T_C$ (T_C is the critical temperature). The ferroelectric thin film system is assumed symmetric and the thickness L extends from $-L/2$ to $L/2$ along the z axis. Two trigonometric trial functions are used to represent approximately the polarization profile within the thin film. The properties of the ferroelectric thin films in the second-order phase transition are studied by using Tilley-Zeks model of the free energy and the Landau-Devonshire free energy expansion. The free energy density is evaluated and calculated to derive the dielectric susceptibility expression. After minimizing the free energy with respect to polarization and using $\chi_T^{-1} = \partial E / \partial P$, the dielectric susceptibility expression is derived. The behavior of dielectric susceptibility χ_T in ferroelectric thin film is studied under the influence of various thicknesses, temperatures and boundary conditions. For case studies, there are two trial functions is taken into consideration, one is for zero surface polarization $P_{\pm} = 0$, and another one is for non-zero surface polarization $P_{\pm} \neq 0$.

The numerical method is also presented to provide further support to the results of calculation. The discrete model is also based on the framework of the Landau-Devonshire free energy expansion in term of polarization. The polarization profile of the thin film is determined and the average polarization is evaluated to calculate the dielectric susceptibility. The results for these two different boundary conditions, zero surface polarization $P_{\pm} = 0$ and non-zero surface polarization $P_{\pm} \neq 0$, are compared with calculated result.

The results have been found that the analytical calculation and the numerical results are accurate in describing the behaviors of the temperature and thickness dependence of the dielectric properties of a second-order FE thin film. It has been demonstrate that the dielectric susceptibility of the FE film is also dependent on the extrapolation length and boundary conditions.

CHAPTER 1

GENERAL INTRODUCTION

1.1 Introduction **Equation Chapter 1 Section 1**

Ferroelectrics (FE) are advanced materials with a lot of technological applications. This kind of materials typically exhibit high dielectric susceptibility, hysteresis, electro-mechanical coupling, electro-optical effect, memory effect and electric displacement. One of the most recent applications of ferroelectrics is as a high power capacitor, based on its dielectric susceptibility property. At the same time, miniaturization of electronic device has been the main driving force for the development of ferroelectric thin film. Therefore, this research has been carried out to study the characteristic of dielectric susceptibility of ferroelectric thin film from the theoretical and numerical aspects in order to understand the characteristic of ferroelectric material under the influence of surface effect. The research presented in this thesis elucidates the study of dielectric susceptibility of ferroelectric thin film by using suitable trial function.

1.2 Motivation of Study

Recently, Prof. Ishibashi has proposed a different way to investigate dielectric susceptibility behaviour of the ferroelectric thin film. In this idea, trial function is used as a presumed polarization profile in order to avoid tedious calculation of elliptic functions which are exact solutions (Ong, 2001). Although it is not the first time proposed in theoretical studies, but only several scientists have used this method to study ferroelectric properties. The dielectric susceptibility of a FE film is calculated by using two different types of trial functions in particular cosine function. The cosine function is chosen because it approximates to the elliptic function when the film is thin in thickness. Two cases are considered, (1) zero surface polarization case, and (2) non-zero surface

polarization case. By using the trial function into the Landau-Ginzburg-Devonshire free energy density, the first derivative with respect to polarization gives the corresponding electric field and the second derivative gives the reciprocal dielectric susceptibility χ^{-1} . The characteristics of the reciprocal dielectric susceptibility χ^{-1} and the dielectric susceptibility χ are presented and discussed in the relation to bulk case.

1.3 Organization of Contents

In the next section of this chapter, a brief history of ferroelectric is given. It is then followed by an explanation and definition for ferroelectricity. A general overview of basic concepts in FE is also presented. In this section, characteristic, classes of ferroelectric materials and applications are elucidated in brief.

In Chapter 2, some literature reviews and important theories in ferroelectricity are presented. The formulation of Landau-Devonshire theory and the calculation of dielectric susceptibility for first and second order ferroelectric in the bulk case are presented. The bulk case results are important to represent the limiting case when the film gets thicker. The results will be used to compare with the thin film cases.

A formalism based on the use of trial functions to approximate the polarization profile for second order phase thin film is shown here in Chapter 3. Calculations of dielectric susceptibility by using two different trial functions are introduced here. The results are shown and discussed.

Chapter 4 presents the formulation of the Landau-Devonshire theory in ferroelectric film. In the subsequent section, the numerical method and the fourth-order Runge-Kutta method are introduced. The numerical results obtained from this numerical work are presented.

Finally, the results of calculation and numerical method of ferroelectric thin film are discussed in chapter 5. Conclusions are drawn and suggestions for future research are also given here.

1.4 Past and Present of Ferroelectricity

The discovery of ferroelectricity resulted from a long history of observation that under certain conditions, some materials could become charged, generate sparks and attract small pieces of paper, wood, etc. In the early 1880s, Pierre and Jacques Curie discovered that some natural crystalline materials, such as quartz, could change shape when subjected to an electric field. This property, named as piezoelectricity, was later also found in some artificial crystals such as ammonium dihydrogen phosphate, lithium sulphate and sodium potassium tartrate tetrahydrate.

In 1894, Pockels found the Rochelle salt, sodium potassium tartrate tetrahydrate ($\text{NaKC}_4\text{H}_4\text{O}_6 \cdot 4\text{H}_2\text{O}$) to exhibit anomalously high piezoelectric effect than most other materials. In 1920, Joseph Valasek discovered that the polarization of Rochelle salt could actually be reoriented by the application of an external electric field below a certain transition temperature. This phenomenon was later called ferroelectricity in solid state physics. Rochelle salt presents ferroelectric phase between 255K and 297K, and higher than this temperature range, it is in the paraelectric phase. By applying external electric field across a cooled sample and tracking the output current, he produced a hysteretic charge loop shown in Fig. 1.1. He also noted that P (polarization) versus E (electric field) was analogous to B (magnetic flux density) versus H (magnetic field intensity). He published the paper with title Piezo-Electric and Allied Phenomena in Rochelle Salt (Valasek, 1920).

In 1935, G. Busch and P. Scherrer discovered the second ferroelectric material potassium dihydrogen phosphate (KDP), KH_2PO_4 . Its isomorphs (ammonium dihydrogen phosphate and potassium dihydrogen arsenate) also contains the properties of ferroelectricity. The first phenomenological theory was proposed by Muller to describe the relations between piezoelectric, anomalous dielectric and elastic

behaviours of the crystal in 1940. In 1941, Slater introduced the theory of phase transition to explain the behaviour of KH_2PO_4 .

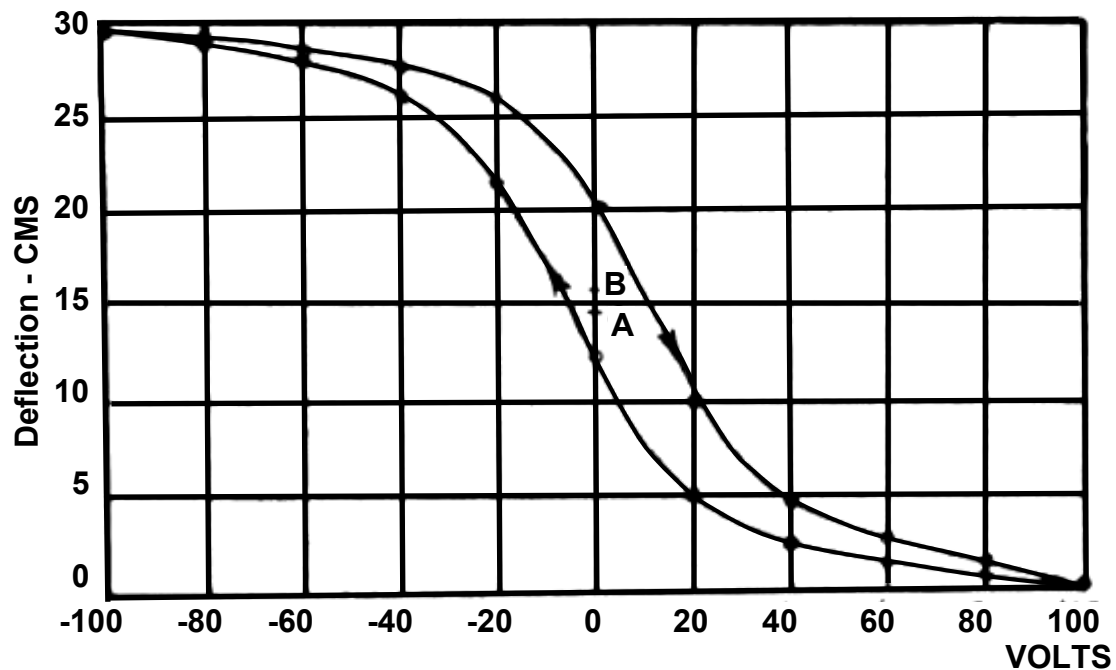


Fig. 1.1. Rochelle salt hysteresis loop obtained by J. Valesek. (Valasek 1920)

The third major ferroelectric substance, barium titanate BaTiO_3 , was discovered after 1940. Many independent researchers in Russia, England, Holland, Japan and Switzerland worked on this material between 1940 and 1945. Wainer and Solomon in the U.S.A., and Wul and Goldman in the U.S.S.R., and Ogawa in Japan independently discovered the anomalous dielectric properties of BaTiO_3 in 1943. In 1946, Wul and Goldman and Von Hippel *et al.* confirmed that BaTiO_3 is ferroelectric. An excellent accounting of this research is given by A. Von Hippel from MIT in a paper published in *Modern Physics* in 1950 (Von Hippel, 1950). Barium titanate was the first ferroelectric material in ceramic form. This proves that ferroelectricity is not only associated with hydrogen bonding (such as found in such water soluble compounds like Rochelle Salt, potassium dihydrogen phosphate, ammonium dihydrogen phosphate, etc.), but also can exist in simple oxide materials. Barium titanate is a member of the

perovskite family. This crystal family category is based on the atomic configuration of the mineral perovskite.

Since the barium titanate discovery, this crystal family has yielded over 250 pure materials and mixed systems that exhibit ferroelectricity. In fact, a vast group of materials possesses spontaneous polarization in the absence of external electric field. It is estimated that there are now approximately 2000 known ferroelectric materials have been discovered. The number of ferroelectric materials has increased rapidly, and now reaches more than two hundred species. In the last forty years, about five or six new ferroelectric materials have been discovered each year. Among the new ferroelectric materials is the mineral fresnoite $Ba_2TiOSi_2O_7$ (Foster *et al.*, 1999) together with a group of isostructural materials including $K_2V_3O_8$, $Rb_2V_3O_8$, $(NH_4)V_3O_8$ and $K_2VOP_2O_7$ (Abrahams, 1996). It is interesting to note that even ice exhibits ferroelectric properties (Nelson and Baker, 2003).

Table 1.1: Important events in ferroelectricity (Cross and Newnham, 2003).

1920-1930	Rochelle salt period: discovery of ferroelectricity
1930-1940	KDP age: Thermodynamic and atomic models of ferroelectricity
1940-1950	Early barium titanate era: High- <i>K</i> capacitors developed
1950-1960	Period of proliferation: Many new ferroelectrics discovered
1960-1970	Age of high science: soft modes and order parameters
1970-1980	Age of diversification: Ferroelectrics, electro-optics, thermistors
1980-1990	Age of integration: Packages, composites and integrated optics
1990-2000	Age of miniaturization: size effect, manipulated modes and dipoles

Recently, due to the application and the rapid progress in the manufacture of capacitor and memory devices in ferroelectric films, there has been a rise of great research interest in ferroelectrics. Many important breakthroughs have been made and given a more comprehensive understanding especially in the areas of the phenomenological theory and calculations, finite size effects, fundamental and

application studies of ferroelectric composites and liquid crystals. Table 1.1 lists a summary of historical events in ferroelectricity (Cross and Newnham, 2003).

1.5 Definition of Ferroelectricity

Ferroelectricity is the phenomenon of a spontaneous polarization which exists in the material at two opposite orientation states and can be reversed by an applied electric field (Grindlay, 1970) as shown in Fig. 1.2. Ferroelectricity is characterized by a polarization-electric field (P - E) hysteresis loop. The spontaneous polarization P_s is the polarization which presents in the ferroelectric crystal in the absence of external electric field. Spontaneous polarization P_s is defined as the surface density of the bound charge on the sample surface (Strukov & Levanyuk, 1998). When temperature is increasing, P_s usually decreases rapidly on crossing the Curie temperature. The value of polarization plotted versus applied electric field for the ferroelectric state shows specific response namely the hysteresis loop.

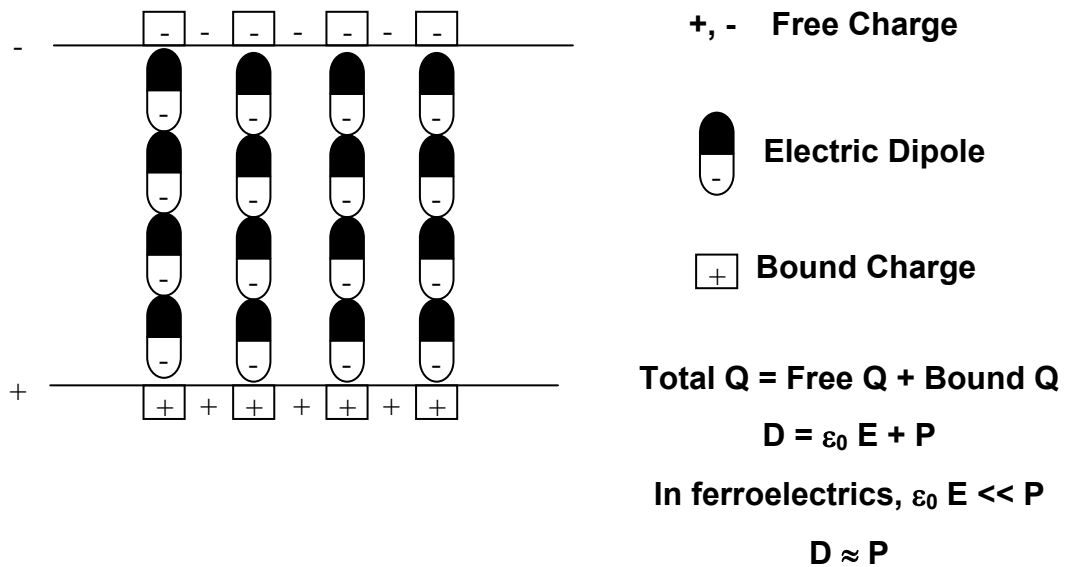


Fig. 1.2: A ferroelectric is a polar material whose spontaneous polarization can be reversed or re-oriented by applying electric field. A simple illustration of a ferroelectric material (figure courtesy of Symetrix Corporation).

1.6 Classification of Ferroelectric Materials

Most of the ferroelectric materials have perovskite structure and many could form solid solutions by adding dopant, such as PLZT is La doped with PZT. Table 1.2 shows some ferroelectric material. Ferroelectric can be divided into two main groups, displacive (polarization along several axes that are equivalent in the unpolar state) and order-disorder (polarization along only one axis, “up” or “down”) (Kanzig, 1957). Table 1.3 gives some common ferroelectric materials.

Table 1.2: Displacive and order-disorder ferroelectric materials (Kittel, 1986)

Transition	Displacive	Order-disorder
Property	If in the paraelectric phase, the atomic displacements are oscillations about a non-polar site, then after a displacive transition the oscillations are about a polar site.	If in the paraelectric phase, the atomic displacements are about double-well or multi-well configuration of sites, then in an order-disorder transition the displacements are about an ordered subset of these wells.
Materials	Ionic crystal structure closely related to the perovskite and ilmenite structures. The simplest ferroelectric crystal is GeTe with the sodium chloride structure.	Crystals with hydrogen bonds in which the motion of the proton is related to ferroelectric properties, as in potassium dihydrogen phosphate (KH_2PO_4 , KDP) and isomorphous salts.

Table 1.3: Some common ferroelectric materials (Auciello, 1998).

Material	Abbrev	Full Name	Lattice constant (A)	CTE($10^6/^\circ\text{C}$)
BaTiO ₃	BT	Barium Titanate	a=b=3.992, c=4.036	
Ba ₄ Ti ₃ O ₁₂			a=5.45, b=5.41, c=32.83	
(Bi ₄ La) ₄ Ti ₃ O ₁₂	BLT	Bismuth Lanthanum Titanate		
Ba _x Sr _{1-x} TiO ₃	BST	Barium Strontium Titanate	a=b=3.904, c=4.152	
PbTiO ₃	PT	Lead Titanate		a=27, c=67
Pb _{1-x} La _x TiO ₃	PLT	Lead Lanthanum Titanate	a=3.9, c=4.1	
PbZr _{1-x} Ti _x O ₃	PZT	Lead Zirconate Titanate		
Pb _{1-x} La _x (Zr _y Ti _{1-y})O ₃	PLZT	Lead Lanthanum Zirconate Titanate		
Pb(Mg _{1-x} Nb _x)O ₃	PMN	Lead Magnesium Niobate		
Pb(Mg _{1/3} Nb _{2/3}) _{1-x} Ti _x O ₃	PMNT (PMN-PT)	Lead Magnesium Niobate with Lead Titanate**		
(1-y)Pb(Zn _{1/3} Nb _{2/3})O _{3-y} PbTiO ₃	PZNT			
SrTiO ₃	ST	Strontium Titanate	a=3.905 ($\sqrt{2}a=5.522$)	a=11
SrBi ₂ Ta ₂ O ₉	SBT	Strontium Bismuth Tantalate	a=5.531, b=5.534, c=24.984	
LiAlO ₃			a=5.356	a=11
LiNbO ₃	LN		a=5.148, c=13.863	
Si			5.432	a=2.6
GaAs			5.65	6.86
SrO			5.14	
MgO			4.211	10.6

1.6.1 Displacive Ferroelectrics

This group of ferroelectric materials exhibits the polarization due to ionic displacements of certain atoms in the crystal lattice dynamics. Fig. 1.3 shows some common elements in the displacive type of ferroelectric crystal. The displacive class crystal contains oxygen octahedra, so it is also named as oxygen octahedral ferroelectrics. The most typical displacive ferroelectrics is perovskite type, for example BaTiO_3 , KNbO_3 , PbTiO_3 , KTaO_3 , NaNbO_3 , NaTaO_3 , PbZrO_3 , PbHfO_3 , LiNbO_3 , LiTaO_3 , etc (Xu, 1991). The generic formula of perovskite type is ABO_3 where “A” represents a monovalent or divalent metal (Ba, Pb, Sr, Ca, Bi, K or Na) and “B” represents tetravalent or pentavalent (Ti, Nb, Zr, Ta, Mo, W and Fe), possible combinations are $\text{A}^{2+}\text{B}^{4+}$ or $\text{A}^{1+}\text{B}^{5+}$.

Common elements for ferroelectric crystals

I H 1	Common elements for ferroelectric crystals																VIIIB He 2	
IIA Li 3	Be 4											IIIB B 5	IVB C 6	VB N 7	VIB O 8	VIIA F 9	Ne 10	
Na 11	Mg 12											Al 13	Si 14	P 15	S 16	Cl 17	Ar 18	
III A K 19	Ca 20	Sc 21	IV A Ti 22	V A V 23	VI A Cr 24	VII A Mn 25	VIII A Fe 26	VIII A Co 27	VIII A Ni 28	IB Cu 29	IIB Zn 30	Ga 31	Ge 32	As 33	Se 34	VII B Br 35	Kr 36	
Rb 37	Sr 38	Y 39	Zr 40	Nb 41	Mo 42	Tc 43	Ru 44	Rh 45	Pd 46	Ag 47	Cd 48	In 49	Sn 50	Sb 51	Te 52	I 53	Xe 54	
Cs 55	Ba 56	La 57	Hf 72	Ta 73	W 74	Re 75	Os 76	Ir 77	Pt 78	Au 79	Hg 80	Tl 81	Pb 82	Bi 83	Po 84	At 85	Rn 86	
Fr 87	Ra 88	Ac 89																
			Ce 58	Pr 59	Nd 60	Pm 61	Sm 62	Eu 63	Gd 64	Tb 65	Dy 66	Ho 67	Er 68	Tm 69	Yb 70	Lu 71		
			Th 90	Pa 91	U 92	Np 93	Pu 94	Am 95	Cm 96	Bk 97	Cf 98	Es 99	Fm 100	Md 101	No 102	Lr 103		

Fig. 1.3: Common elements, marked in shaded area, in the displacive type of ferroelectric crystal (Richerson, 1992).

A perovskite has a cubic crystal structure in the high-temperature phase (Fig. 1.4). “A” atoms are usually a large positive ions and reside at eight corners of the cubic lattice, “B” atoms reside at the body centre, while oxygen atoms position at the face

centres. The whole structure is formed by linking the vertices of the oxygen octahedral. The cavities are mainly occupied by the “A” atoms. The oxygen octahedron has three fourfold axes, four threefold axes and six twofold axes. The polarization occurs when “B” is displaced from the cubic centre along any of these symmetry axes.

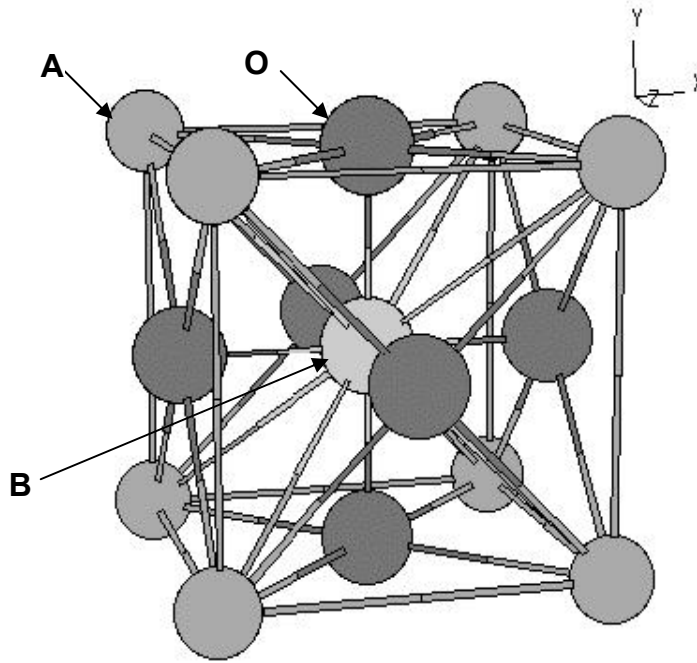


Fig. 1.4: Lattice with perovskite structure having formula ABO_3 . “A” atom, “B” atom, and oxygen occupy the corner site, body-centered site, and face-centered site, respectively (A.F Wells, 1995).

Barium titanate $BaTiO_3$ is the first discovered ferroelectric material of perovskite type and becomes the most common example for studies. Above $120^\circ C$, it is in paraelectric phase and has simple cubic structure with space group $Pm3m$. When temperature is below $120^\circ C$, it will transform into three ferroelectric phases. First, it transforms to $P4mm$ tetragonal along a fourfold axis, then to $Amm2$ orthorhombic at about $0^\circ C$ along a twofold axis and finally to $R3m$ trigonal phase below $-70^\circ C$ along a threefold axis as shown in Fig. 1.5. The polar axes in the three ferroelectric phases are $[001]$, $[011]$ and $[111]$ respectively. All these are the first order phase transitions with discontinuities in the dielectric constant, which follows the Curie-Weiss Law

$\epsilon \propto (T - T_0)^{-1}$. A detailed account of other properties of BaTiO₃ is available in Jona and Shirane (1962).

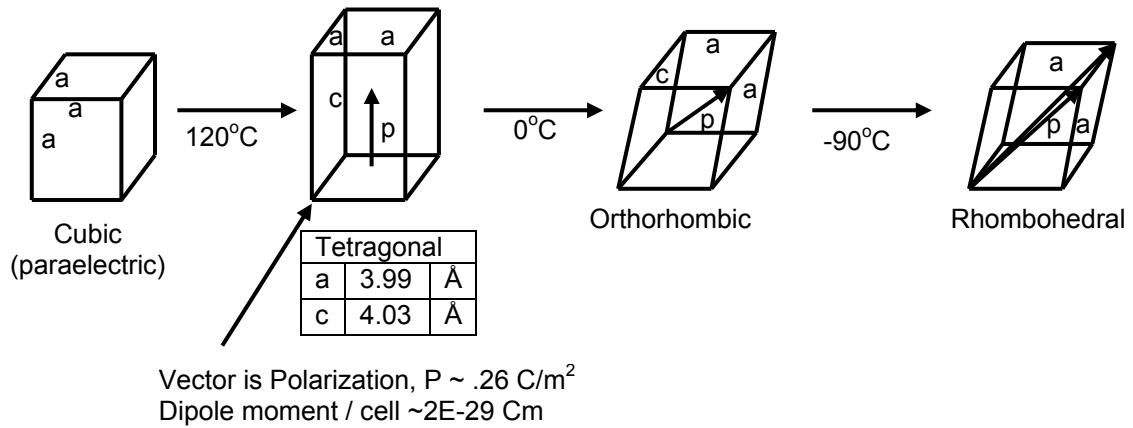


Fig. 1.5: Different symmetry axes directions (A.F. Wells, 1995).

The crystal structure of PbTiO₃ is shown in Fig. 1.6 (Damjanovic, 1998). In paraelectric phase, Pb, O and Ti atoms occupy corners, face centred and body centred sites of cubic respectively. At room temperature, the tetragonal crystal structure has the ionic displacement which is parallel in the polar phase of the oxygen octahedral during para-ferro phase transition (Shirane *et al.*, 1956). During the phase transition, the oxygen atoms and “B” cations in PbTiO₃ shift in the same direction relative to the “A” cations. Pb atoms possess larger size compared to Ti atoms in the octahedral interstitial position, so Ti ions have small margin of stability. Thus, the minimum energy can only be reached if Ti ion position is off-centred in surrounding of six oxygen ions as illustrated in Fig. 1.6. The random position of Ti ion in one of these six possible minimum energy sites will result the spontaneous polarization.

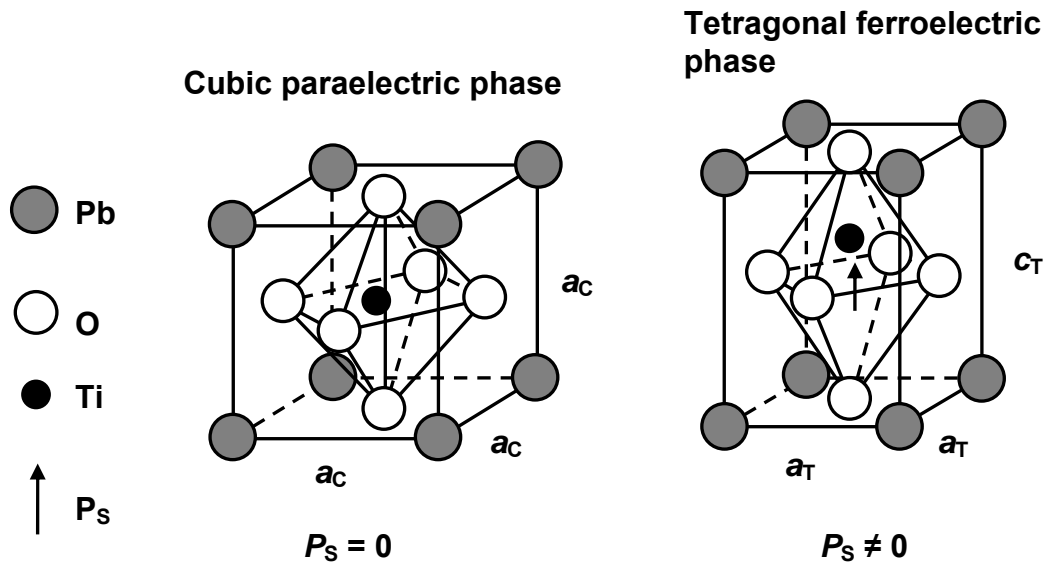


Fig. 1.6: The perovskite structure ABO_3 of $PbTiO_3$ in a) paraelectric and b) ferroelectric phase (Damjanovic, 1998).

1.6.2 Order-Disorder Ferroelectrics

The order-disorder class of ferroelectrics includes crystals in which the spontaneous polarization is a result from the linear ordering of the proton ions in the structure. There are two major groups of order-disorder ferroelectrics. The first one consists of elements, such as phosphates, sulphates, fluoroberyllates, cyanides, periodates and glycine compounds, where the spontaneous polarizations appears as a result of the ordering of protons in the hydrogen bonds. They are known as hydrogen-bonded ferroelectrics. The second group consists of tartrates, potassium nitrate, sodium nitrate, dicalcium strontium propionate and tetramethylammomium chloro- and bromomercurates. In this group, spontaneous polarization is caused by the arbitrary ordering of radicals, which takes place from hindered rotation.

The typical examples of order-disorder ferroelectrics are sodium nitrite $NaNO_2$, potassium dihydrogen phosphate (KDP) KH_2PO_4 and triglycine sulphate (TGS) $(CH_2NH_2COOH)_3 H_2SO_4$. KDP is tetragonal above 124K with a non-centrosymmetric space group $\bar{1}42d$. Below 124K, it is in orthorhombic ferroelectric phase with space

group $Fdd2$. The key part of the crystal structure is three dimensional network of PO_4 groups linked by the $O-H\cdots O$, hydrogen bonds to the adjacent PO_4 group. Two upper atoms of one PO_4 tetrahedron are joined to the lower oxygen atoms of two other tetrahedron, while two lower oxygen atoms of the tetrahedron are joined to the upper oxygen atoms of another two tetrahedron (Zhong, 1996, 1998, Lines and Glass, 1997 and Zheludev, 1971). The schematic representation of KDP is shown in Fig. 1.7.

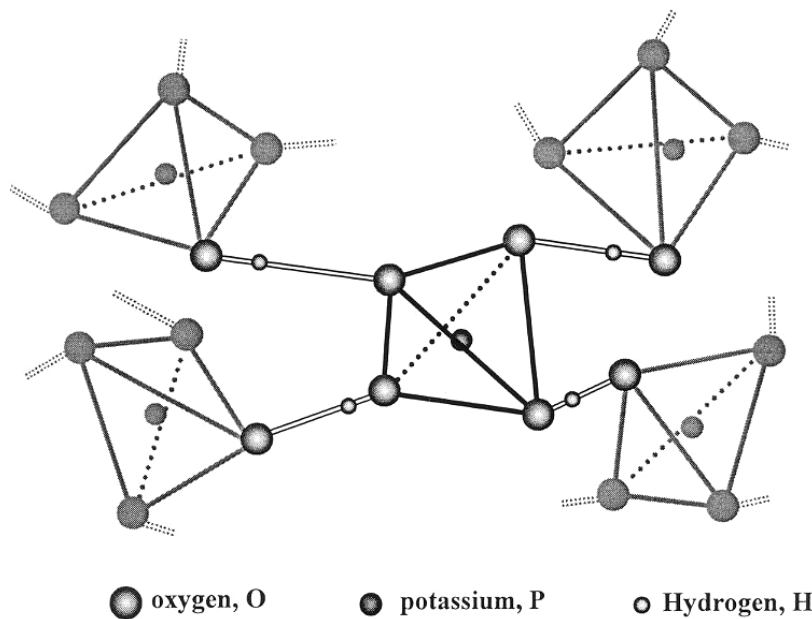


Fig. 1.7: Schematic diagram of the hydrogen bond system in KH_2PO_4 (KDP) crystals. The PO_4 groups with hydrogen bonds link to the nearest PO_4 groups (Zhong, 1998).

The ordering of proton in a hydrogen bond produces an internal field that displaces atom P and causes dipole moments exists in the PO_4 groups. The ordering then displaces potassium atom, and contributes additionally to polarization. A proton of the hydrogen bond can be represented as a double-well potential. The proton sits in one of the wells and the bonding energy is the same in either way. Above T_c , the proton distribution in the potential wells is disordered and random between the two equilibrium positions along the bond length. However, below T_c , the distribution becomes ordered. There will be a larger fraction of protons in one side of the well than the other one. When the spontaneous polarization increases with the degree of

ordering of these protons, the hydrogen ion does not contribute to the spontaneous polarization because the displacement in hydrogen bond is perpendicular to the ferroelectric axis. However, the ordered state of proton induces displacements of K, P along the c -axis that causes the dipole moment. The basic theoretical model of the order-disorder ferroelectrics is a pseudo-spin Hamiltonian with the Ising Model in a Transverse Field (Lines and Glass, 1977).

1.7 Properties of Ferroelectric materials

1.7.1 Hysteresis Loop and Polarization Switching

One of the main characteristics of ferroelectric materials is the polarization switching or reversal when an external electric field is applied to the crystal. The changes of polarization can be observed experimentally in the variation of the electric field applied to the crystal by using a Sawyer-Tower circuit as shown in Fig. 1.8 (Sawyer and Tower, 1969). An electric field E is applied to the crystal, which varies periodically in the same way of electric voltage U . As a consequence of electric field variation, the polarization switching occurs and ferroelectric hysteresis loop is observed.

When an electric field is applied to a ferroelectric crystal, the polarization increases linearly with the field strength along OA as shown in Fig. 1.9. In this region, the applied electric field is not strong enough to reverse domains. As the field strength increases the polarization of the domains with unfavourable orientation one starts to reverse. A redistribution of the volumes of energetically favourable and unfavourable domains occurs (region AB). A further increase in the electric field strength causes all the domains to align in the same direction as the field, point C. If the applied field strength slowly decreases, some domains will back-switch. At zero-field point D, the polarization is nonzero. The crystal reaches a zero polarization state at point E, as the

external field is reversed. Further increase of the field in the negative direction results in a new reorientation of the dipole moments reaching saturation at point F, with the polarization in the opposite direction to that at point C. At point D, when the applied electric field is absent, the remained nonzero polarization is called the remnant polarization, P_R . The linearly extrapolated value from point C that gives the saturation polarization is referred to as the spontaneous polarization P_S of the crystal. The coercive field E_c is the minimum electric field applied at the opposite direction to cancel the spontaneous polarization and make the polarization start to switch in the crystal. In the ferroelectric hysteresis loop of a PbTiO_3 single crystal, spontaneous polarization equals to $52 \mu\text{C}/\text{cm}^2$ and coercive field equals to $6.75 \text{ kV}/\text{cm}$ (Strukov & Levanyuk, 1998). When the applied field reaches E_c , reversal or switching of the direction of polarization begins.

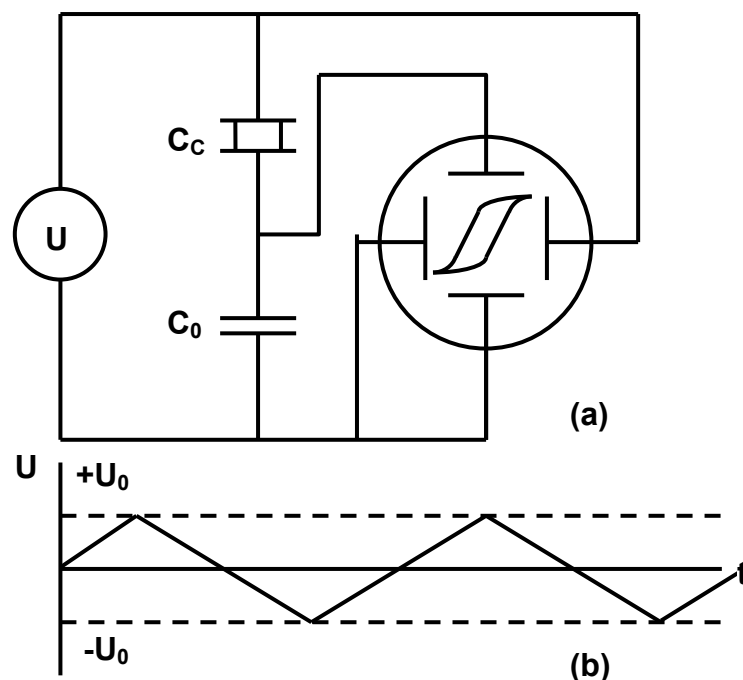


Fig. 1.8: a) the simplest electric circuit for observation of the dependence of electric polarization on electric (Sawyer-Tower circuit) and b) the shape of voltage applied to crystal (Sawyer and Tower, 1969).

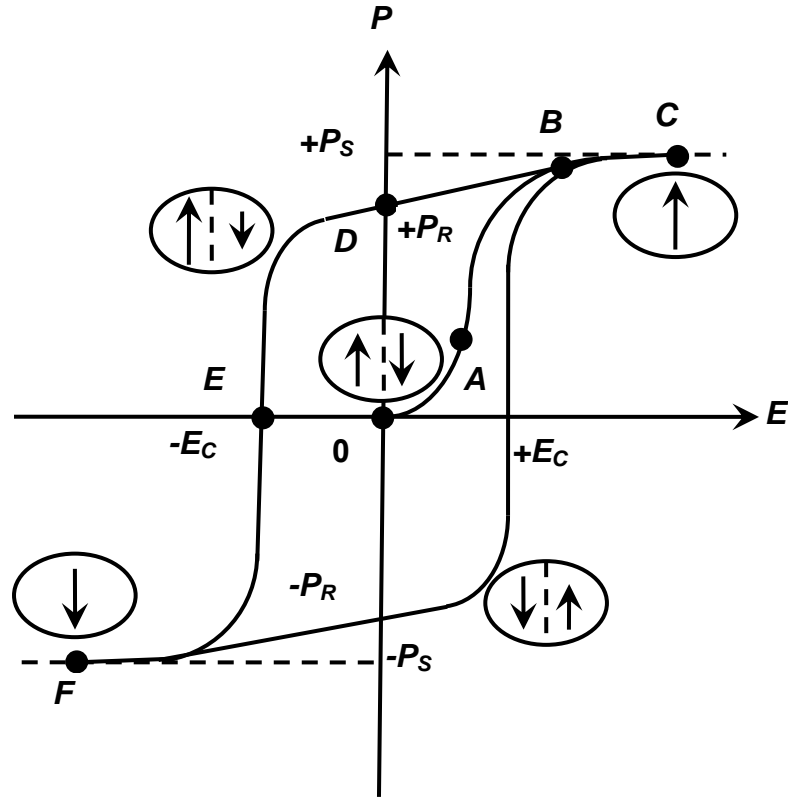


Fig. 1.9: Schematic illustration of the P - E hysteresis loop. Ellipses with arrows show the polarization of the crystal (Sawyer and Tower, 1969).

Polarization reversal is a consequence of the motion of domain walls under the influence of the applied field. It is a nucleation growth mechanism which takes place inhomogeneously throughout the crystal. The mechanism can be mainly categorized into four stages as shown in Fig. 1.10: formation of new domains, forward movement of domains, and sidewise movement of domain walls and coalescence of domains.

In general, an ideal hysteresis is symmetrical in shape so that $|+E_C| = |-E_C|$ and $|+P_R| = |-P_R|$. The shape of the loop, coercive field, spontaneous polarization and remnant polarization is affected by factors such as finite size, defects and stresses or strains. Switching current data provides information on nucleation, growth and coalescence of domain (Shur, 1996). Most theoretical model is partly based on the classical Kolmogorov-Avrami theory of the crystalline growth. Subsequently domain switching is adapted in ferroelectrics as introduced by Ishibashi and Takagi (1971).

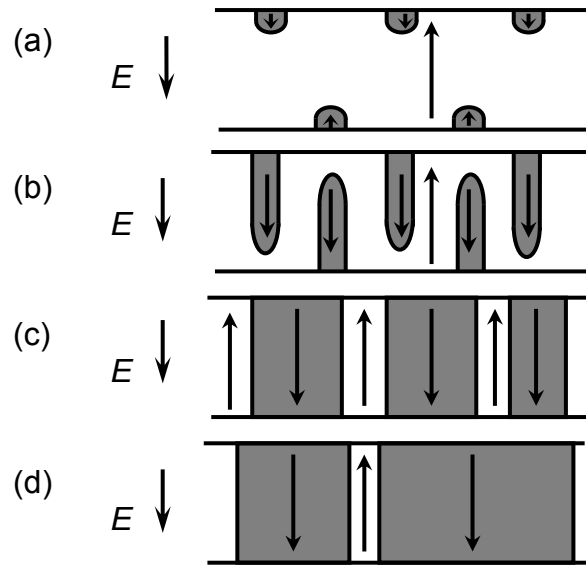


Fig. 1.10: Schematic illustration of the nucleation and growth process during polarization switching (Chew, 2001).

1.7.2 Dielectric and Susceptibility

From Fig. 1.9, the gradient of the hysteresis loop connecting E and P equals to the electric susceptibility χ_T . The susceptibility of a material or sustains describes the variation of polarization which response to the changes in the applied field:

$$P = \chi \epsilon_0 E = (\epsilon_r - 1) \epsilon_0 E \quad (1.1)$$

$$\chi = \epsilon_r - 1 \quad (1.2)$$

And also,

$$\chi \epsilon_0 = \frac{\partial P}{\partial E} \quad (1.3)$$

$$\chi_T = \frac{\partial P}{\partial E} \quad (1.4)$$

In ferroelectric material, the value of dielectric constant or susceptibility varies with the changes of temperature. The temperature dependence of dielectric constant $\epsilon(T)$ is shown in Fig. 1.11. The transition from ferroelectric phase to paraelectric phase is accompanied by dielectric constant anomaly.

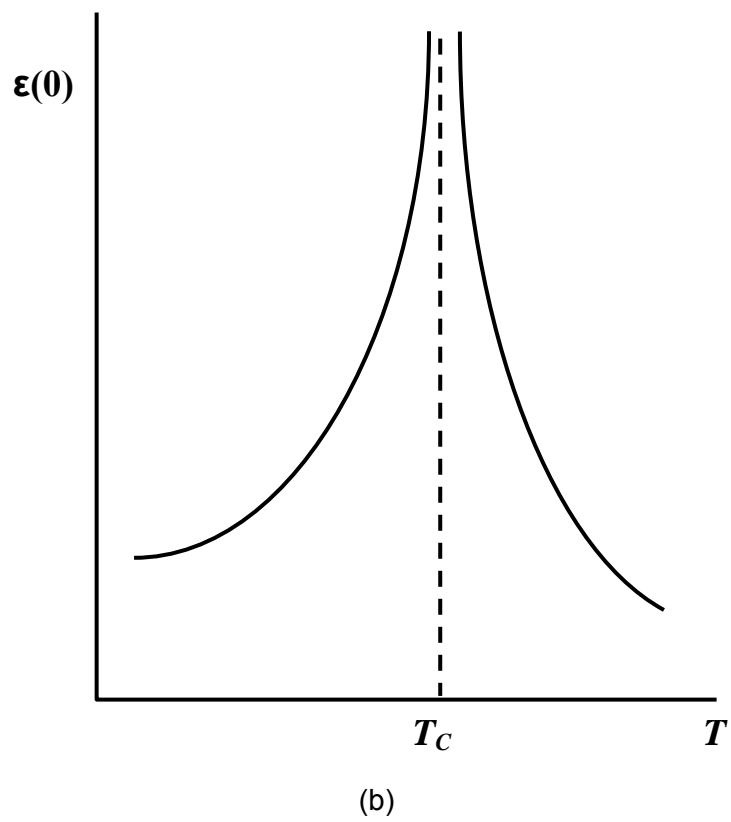
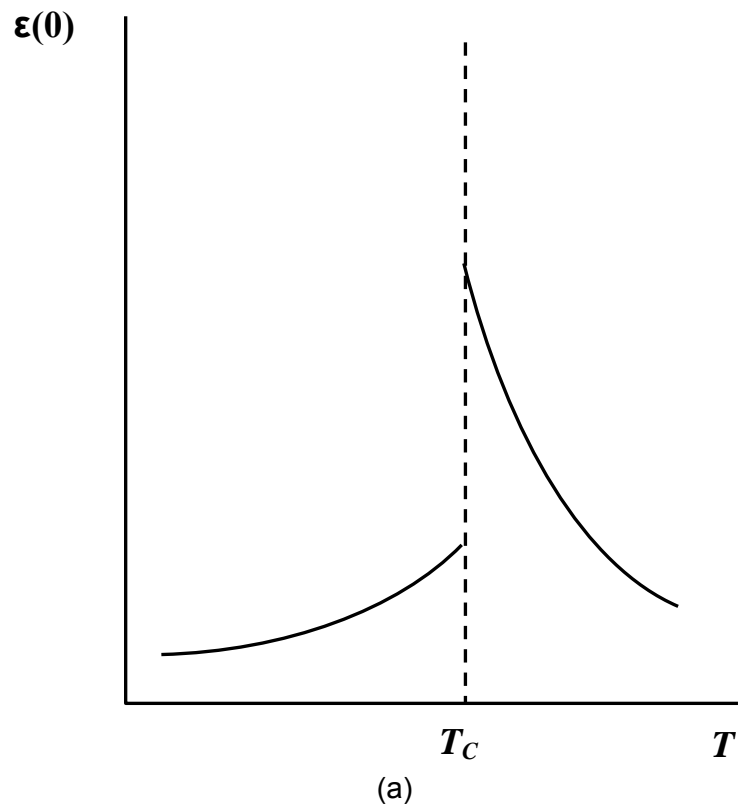


Fig. 1.11: Temperature dependence of $\varepsilon(T)$ a) first order transition and b) second order transition.

One of ferroelectrics properties is high dielectric constant. The temperature dependence of $\epsilon(T)$ in the paraelectric phase has the form of the Curie-Weiss Law and which $\epsilon(T)$ diverges and exhibits a singularity at temperature T_0 :

$$\epsilon(T) = \frac{C}{T - T_0} \quad (1.5)$$

where C is the Curie constant and the Curie-Weiss temperature $T_0 = T_C$ for the second order transition, but $T_0 \neq T_C$ for the first order transition. Extremely large values of dielectric constant e.g. $\epsilon(T) \approx 10^4$, are achieved at the ferroelectric transition. Fig. 1.12 schematically shows the temperature variation of the dielectric constant of BaTiO₃. The Curie point for BaTiO₃ is 120°C. Other materials have the ferroelectric properties which are identical to BaTiO₃, except the Curie point are different, for example: PbTiO₃ ($T_C = 490^\circ\text{C}$), KNbO₃ ($T_C = 435^\circ\text{C}$), KTaO₃ ($T_C = -260^\circ\text{C}$).

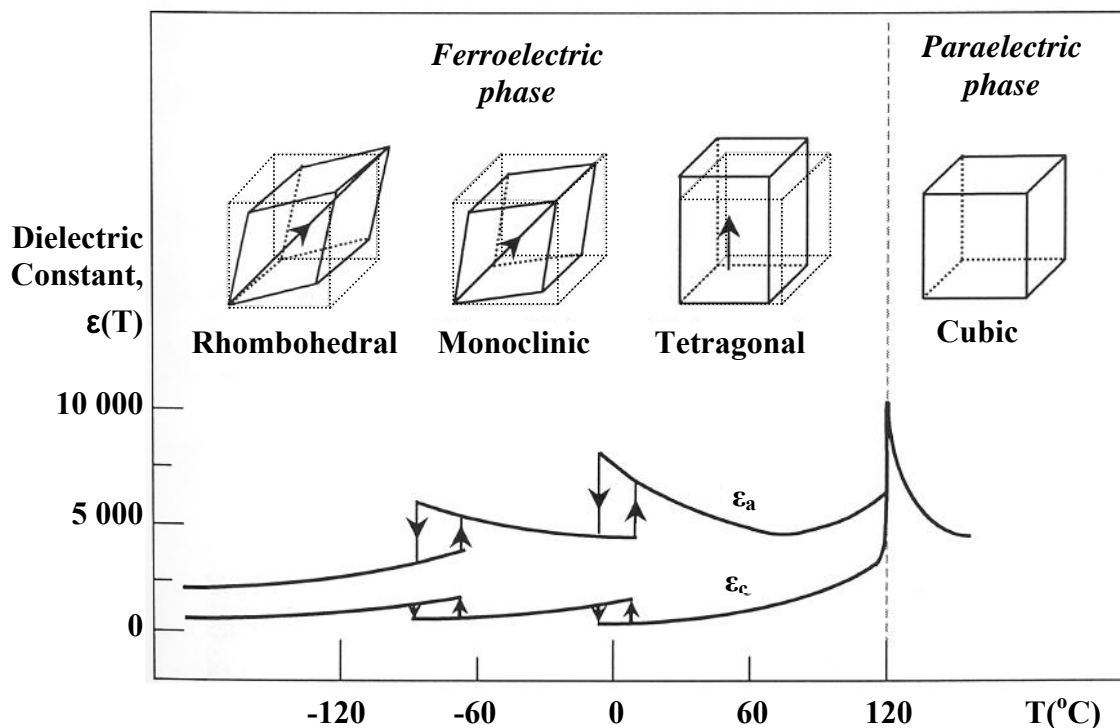


Fig. 1.12: The dielectric constant $\epsilon(T)$ of BaTiO₃ crystal. ϵ_c is the dielectric constant along the polar axis and ϵ_a perpendicular to the axis (Uchino, 2000)

1.7.3 Domains

Usually, a ferroelectric crystal does not have polarization in single direction only. When temperature decreases and becomes lower than the Curie temperature, in the absence of external electrical field and mechanical stress, many small regions known as domains will form inside the crystal. Ferroelectric domain is the region within each of which the polarization align in the equal orientation but in adjacent domains, the polarizations is in different directions (Kittel, 1986). The sum of all different oriented dipoles in all domains gives the resultant polarization. A single crystal that contains no domains is considered as in a single-domain or mono-domain state. The single-domain state in single crystal of ferroelectric materials can be achieved by poling (polarization reversal in strong electric field) shown in Fig. 1.13.

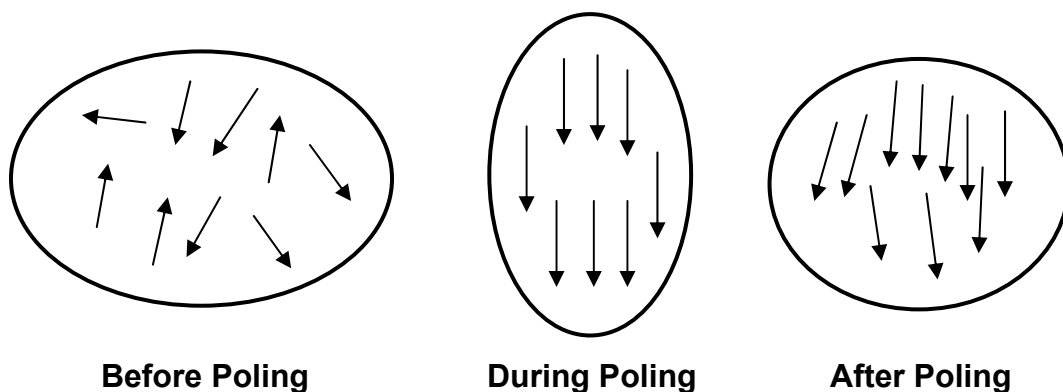


Fig. 1.13: Effect of poling on dipole orientation (Damjanovic, 1998).

The area between two adjacent domains is called domain wall, with thickness in a range of a few lattice constants. Domain walls in ferroelectric materials are much narrower compared to domain walls in ferromagnetic materials. By using the technique of transition electron microscopy (TEM), domain wall in ferroelectric thin film is observed to be in the order of 1~10 nm. In weak to moderate electric field, movement of domain wall makes the extrinsic (non-lattice) contribution to the dielectric, elastic and piezoelectric properties of ferroelectric materials and comparable to the intrinsic effect of the lattice. Domain walls become pinned or clamped by the imperfections and defects. Domain wall pinning defects include oxygen vacancies and electrons trapped

in the domain-wall area. Domain wall displacement is affected by the grain size, dopant, crystallographic orientation and crystal structure, external stresses, electric fields and preparation conditions of ceramics and thin films. Other experimental techniques to study domain structures include powder method, chemical etching, optical birefringence and electron microscopy (Lines and Glass, 1977 and Zhong, 1996).

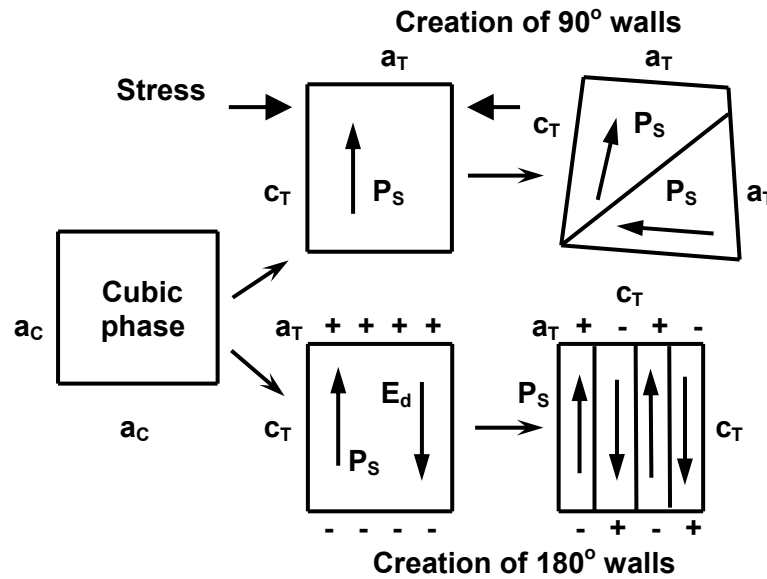


Fig. 1.14: Formation of and domain wall in a tetragonal perovskite ferroelectric phase (Damjanovic, 1998).

At transition temperature, the spontaneous polarization forms surface charges and stray charges accumulate on the surface of ferroelectric material. When there is non-homogeneous distribution of the spontaneous polarization, the surface charge produces an electric field, denoted as depolarization field E_d which is in the opposite direction to the spontaneous polarization (Fig. 1.14). Depolarization field will disturb the stability of single domain state ferroelectrics (Shur, 1996). When the ferroelectric splits into domains with opposite directions and minimize the electrostatic energy associated with the depolarization field. This means the reduction of the energy of the depolarization field formed upon cooling through the ferroelectric phase transition point. Similar to ferromagnetic, the splitting of a ferroelectric crystal into many domains

minimizes the energy and stabilizes the whole system. Formation of domains in a ferroelectric crystal may be also caused an influence of mechanical stresses (Damjanovic, 1998).

The types of domain wall in a ferroelectric crystal depend on the symmetry of both non-ferroelectric and ferroelectric phases of the crystal (Fousek and Janovec, 1969). The polarizations in adjacent domains always make a definite angle between each other. When a crystal is cooled from the paraelectric phase to ferroelectric phase, at least two equivalent directions along the spontaneous polarization may occur. A system with two possible orientations of polarization, such as triglycine sulphate, KH_2PO_4 and Rochelle salt has anti-parallel domains. For systems with more than two possible orientations of the dipoles, a more complicated domain structure may occur. For example, BaTiO_3 in the tetragonal phase with six possible directions of polarization can contain both 180° and 90° domains and the corresponding walls. However in the monoclinic and rhombohedra phases, 60° walls occur in addition to 90° and 180° walls. In BaTiO_3 , the 180° domain wall thickness is estimated to be in range of 0.5-2.0 nm, whereas it is 0.5-10.0 nm for 90° domain wall (Zhong, 1998). Simple diagrams of 180° and 90° domains and the corresponding domain walls are shown in Fig. 1.15.

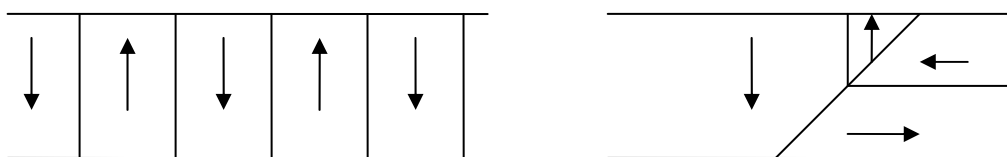


Fig. 1.15: A simple sketch of domain walls: (a) 180° (b) 90° (Zhong, 1998).

Domains also give contribution in polarization switching in ferroelectric crystal. An applied electric field can then switch these domains from one orientation state to another, just as in ferromagnetics. The switching from one domain orientation to another involves work performed on the material, and so the free energy must change

from one state to the other (Burns, 1970). The reversible polarization is accompanied either by domain wall motion (the growth of existing domains anti-parallel to the applied field) or by the nucleation and growth of new anti-parallel domains. More information on this subject is given by Ishibashi (2005).

1.7.4 The Phase Transition

Another important characteristic of ferroelectric is structural phase transition from the paraelectric phase into the ferroelectric phase. The phase transition of ferroelectric is generally a structural phase transition where the spontaneous polarization appears as the order parameter below the transition temperature. Commonly, ferroelectric materials undergo a structural phase transition from random paraelectric phase at high temperature into ordered ferroelectric phase at low temperature. When the temperature decreases, the spontaneous polarization will vanish at a characteristic temperature, named as Curie point or Curie temperature T_c at which the phase transition takes place. When temperature is higher than the Curie temperature $T > T_c$, the material is in the paraelectric phase and the polarization equals to zero. When temperature is lower than the Curie temperature $T < T_c$, the material is in the ferroelectric phase with a non-zero polarization. When the temperature is in the vicinity of the Curie point, the ferroelectric materials show anomalies in the dielectric, elastic, thermal and other thermodynamic properties (Lines, 1977) and is accompanied with changes in the dimensions of the crystal unit cell (Damjanovic, 1998). For example, the dielectric constant in most ferroelectric crystals has an abnormally large value (up to $10^4 \sim 10^5$) near T_c (Xu, 1991). This phenomenon is usually called “dielectric anomaly” and considered to be the basic feature of ferroelectric materials.

There are two categories of ferroelectric phase transition: the first order and the second order. The first order phase transition is the phase transition in which a

discontinuous change in the polarization at the phase-transition temperature as shown in Fig. 1.16(a) occurs. The first order phase transition is also accompanied by a discontinuous change in volume and entropy. Fig. 1.16(b) shows the second order phase transition in which the polarization changes continuously with respect to temperature. The second order phase transition is a continuous transition where the characteristics of the material, such as entropy, density and volume, undergo a continuous change at the phase transition point.

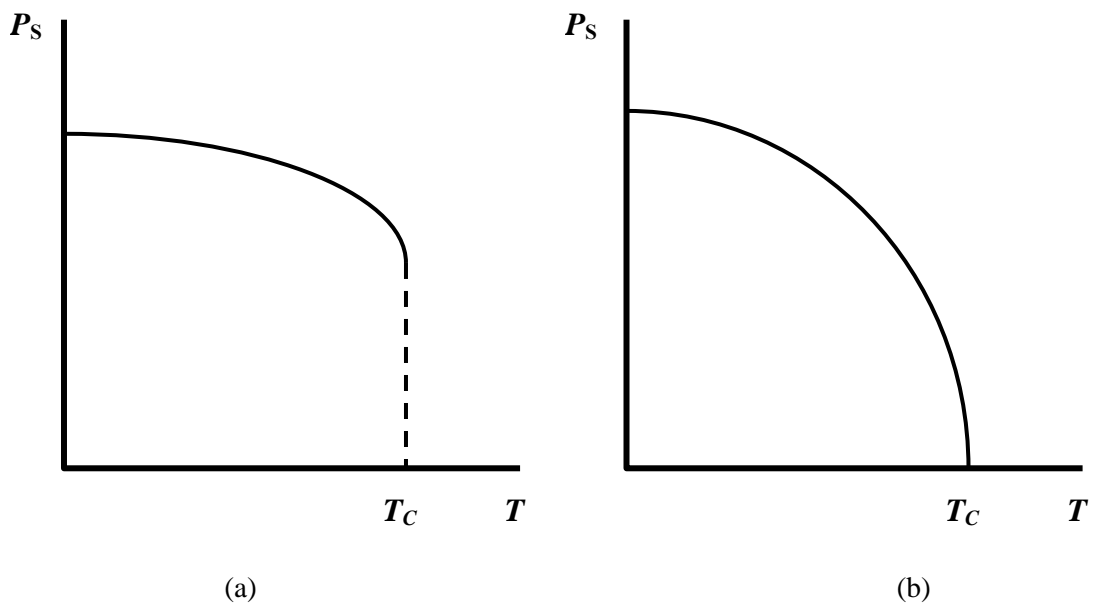


Fig. 1.16: Ferroelectric phase transitions in the vicinity of the Curie temperature T_C . The temperature dependence of P_S : (a) first-order transition and (b) second-order transition (Binc and Zeks, 1974).

In the high temperature paraelectric phase, there is no spontaneous polarization. In Fig. 1.17, spontaneous polarization appears at temperature below 120°C ; upon further cooling, the crystal undergoes another two phase transition at 0°C and -70°C . The transition from cubic phase to tetragonal occurs at 120°C , tetragonal to monoclinic at 0°C and monoclinic to rhombohedral at -70°C . All the transitions in BaTiO_3 crystal are the first order phase transition, except the transition from the cubic perovskite phase to the tetragonal phase, which is the second order phase transition.